



Original Paper

Well interference evaluation considering complex fracture networks through pressure and rate transient analysis in unconventional reservoirs



Jia-Zheng Qin^{a, b}, Qian-Hu Zhong^a, Yong Tang^{a, *}, Wei Yu^b, Kamy Sepehrnoori^b

^a State Key Laboratory of Oil and Gas Reservoir Geology and Exploitation, Southwest Petroleum University, Chengdu 610500, Sichuan, China

^b The University of Texas at Austin, Austin, TX, 78703, USA

ARTICLE INFO

Article history:

Received 8 May 2022

Received in revised form

21 September 2022

Accepted 24 September 2022

Available online 29 September 2022

Edited by Yan-Hua Sun

Keywords:

Well interference

Numerical rate transient analysis

Numerical pressure transient analysis

Complex fracture networks

Embedded discrete fracture model

ABSTRACT

Severe well interference through complex fracture networks (CFNs) can be observed among multi-well pads in low permeability reservoirs. The well interference analysis between multi-fractured horizontal wells (MFHWs) is vitally important for reservoir effective development. Well interference has been historically investigated by pressure transient analysis, while it has shown that rate transient analysis has great potential in well interference diagnosis. However, the impact of complex fracture networks (CFNs) on rate transient behavior of parent well and child well in unconventional reservoirs is still not clear. To further investigate, this paper develops an integrated approach combining pressure and rate transient analysis for well interference diagnosis considering CFNs.

To perform multi-well simulation considering CFNs, non-intrusive embedded discrete fracture model approach was applied for coupling fracture with reservoir models. The impact of CFN including natural fractures and frac-hits on pressure and rate transient behavior in multi-well system was investigated. On a log–log plot, interference flow and compound linear flow are two new flow regimes caused by nearby producers. When both NFs and frac-hits are present in the reservoir, frac-hits have a greater impact on well #1 which contains frac-hits, and NFs have greater impact on well #3 which does not have frac-hits. For all well producing circumstances, it might be challenging to see divergence during pseudosteady state flow brought on by frac-hits on the log–log plot. Besides, when NFs occur, reservoir depletion becomes noticeable in comparison to frac-hits in pressure distribution.

Application of this integrated approach demonstrates that it works well to characterize the well interference among different multi-fractured horizontal wells in a well pad. Better reservoir evaluation can be acquired based on the new features observed in the novel model, demonstrating the practicability of the proposed approach. The findings of this study can help for better evaluating well interference degree in multi-well systems combining PTA and RTA, which can reduce the uncertainty and improve the accuracy of the well interference analysis based on both field pressure and rate data.

© 2022 The Authors. Publishing services by Elsevier B.V. on behalf of KeAi Communications Co. Ltd. This is an open access article under the CC BY-NC-ND license (<http://creativecommons.org/licenses/by-nc-nd/4.0/>).

1. Introduction

Multi-fractured horizontal wells (MFHWs) have become a popular method for the exploitation and development of unconventional reservoirs. Pressure transient analysis (PTA) and rate transient analysis (RTA) have gained tremendous attention since they can help engineers understand the reservoir and fracture

properties (Al-Kabbawi, 2022). Due to the small well spacing and complex fracture networks (CFN) in unconventional reservoir, well interference becomes a severe challenge in PTA and RTA.

In some situation, frac-hits that parent well is affected by the pumping of fracturing treatment of child wells could have strong influence on pressure and rate transient behavior during shale reservoir development (Guindon, 2015; Jacobs, 2017; Sardinha et al., 2014; Wei et al., 2019). The performance of two MFHWs completed in Wolfcamp was studied combining a static discrete fracture network (DFN) and a dynamic reservoir simulation model, which provided a better description of different types of fractures

* Corresponding author.

E-mail address: tangy@swpu.edu.cn (Y. Tang).

including induced, inflated and natural fractures (Ajayi et al., 2016; Mohammed et al., 2020). Through field-scale cases of multi-well shale reservoirs, it has been demonstrated that embedded discrete fracture model (EDFM) is a practical technique with high efficiency and flexibility for studying CFN (Fiallos et al., 2019; Qin et al., 2022; Xu et al., 2018). Furthermore, this technology was further applied to perform shale gas production, in which hydraulic fractures (HFs) and non-uniform distributed natural fractures (NFs) have been considered in the CFN model (Yu et al., 2018, 2019). In detail, the influence of fracture parameters (e.g. HF conductivity and intensity of NFs) and reservoir properties were discussed. Besides, Tang et al. (2019) investigated the effect of an infill well on a parent well using a newly developed compositional reservoir model, in which fractures introduced by infill wells are simulated based on EDFM method.

Interference test was introduced into petroleum engineering for estimating inter-well connectivity by (Elkins, 1953). To improve the accuracy of pore volume reserve and reservoir parameters evaluation, Driscoll (1963) proposed a well interference method suitable for both large and small reservoirs. Malekzadeh and Tiab (1991), Malekzadeh (1992) worked on the solution for horizontal well interference welltest in anisotropic medium for the first time. From 1990s, numerous interference PTA models and loglog curves have been reported for horizontal wells in different conditions (Al-Khamis et al., 2001; Houali and Tiab, 2005; Issaka and Ambastha, 1997; Zhuang, 2012). To better understand the well performance of multiwell-pad-production scheme, researchers developed models for flow regime analysis (He et al., 2020; Qin et al., 2019; Xiao et al., 2018). Nowadays, fracture connection between adjacent wells are commonly seen in the development of unconventional reservoirs. The interference effect caused by fracture-hit connection on pressure transient response is analyzed on the basis of DFN (Wang et al., 2018). For interference test of wells connected by a large fracture, an one-dimensional analytical solution is derived and it shows that the crossflow from the matrix to the fracture cannot be neglected (Gao et al., 2019). Chen et al. (2020) proposed a semi-analytical model analyzing the bottom-hole pressure (BHP) of a child well considering CFN. In his work, CFN includes orthogonal fractures of parent well and child well, also parallel fractures of child well. Some of them are connected through hitting fractures. To detect the interaction between HF and NF, Xiao et al. (2017) developed a semianalytical model and results show that it depends on whether the “dip” shape exists on type curves. The pressure and rate interference response between wells in different layers in Jiaoshiba shale gas reservoir are analyzed by Gao et al. (2020). The HF are surrounded by a dual medium SRV region, represented for fracture networks. Some researchers have also devoted to RTA in multi-well system. Nobakht and Clarkson (2012) explained that the RTA for a group of MFHW is useful for diagnosing the communication between different wells, and engineer could optimize frac job and well spacing based on these results. Subsequently, Lawal et al. (2013) developed an RTA model in shale gas reservoir considering frac-hits and applied it to two plays, Haynesville Shale and Marcellus Shale. Yadav and Motealleh (2017) developed RTA model for studying frac-hits and refracs and applied it to Eagle Ford shale.

Traditional well interference analysis requires the wells to be shut in for obtaining pressure build-up data, and frac-hits and discrete NF in multi-well pads are hardly considered in most previous studies. There is still lack of integrated model combing PTA and RTA model considering frac-hits and discrete NF in multi-well pads. The aim of this work is to propose an integrated approach for evaluating well interference in a multi-well system combing PTA and RTA. In this work, well interference could be diagnosed during producing, which means there is no need for wells to shut in and

well production will not be affected during the interference analysis. Besides, since the wells keep open, pressure and rate data could be recorded and analyzed together, which could effectively reduce the interpretation uncertainty and non-uniquity. Furthermore, the CFN including frac-hits and discrete NF in multi-well pads are taken into consideration during the model establishment.

In this paper, first, non-intrusive embedded discrete fracture model approach was applied for coupling fracture with reservoir models. Then it was investigated that impact of CFN including natural fractures and frac-hits on pressure and rate transient behavior in multi-well system, and analyzed the different flow regimes when parent well produces and all wells produce. Finally, the well-to-well interference was studied and diagnosed. Case study indicates reliable reservoir evaluation results can be acquired based on the new features observed in the novel model, demonstrating the practicability of the proposed approach. The flowchart of this study is shown in Fig. 1.

2. EDFM technology

The non-intrusive EDFM technology has been applied to various studies in recent years since it is flexible and reliable in simulating reservoirs with CFN (Fiallos et al., 2019; He et al., 2022; Miao et al., 2018; Tripoppoom et al., 2019; Xu and Sepehrnoori, 2019; Xu et al., 2018; Yu et al., 2019, 2018). HFs and NFs in physical domain can be discretized into small segments, and virtual grids will be generated in computational domain accordingly by using EDFM. The general sketch of the issue under study is shown in Fig. 2.

Non-neighboring connection (NNC) will be utilized instead of the automatically generated connections by the simulator. NNC can be categorized into several types, including connections between different fracture segments within one fracture or from intersecting fractures, and connections between fracture and matrix. The transmissibility factors are as follows (Xu, 2015; Xu et al., 2017)

$$T_{\text{fracture-matrix}} = \frac{2A_f(K \cdot n) \cdot n}{\int x_n dV} \quad (1)$$

$$T_{\text{individual fracture}} = \frac{\frac{k_f A_c}{d_{\text{seg1}}} \cdot \frac{k_f A_c}{d_{\text{seg2}}}}{\frac{k_f A_c}{d_{\text{seg1}}} + \frac{k_f A_c}{d_{\text{seg2}}}} \quad (2)$$

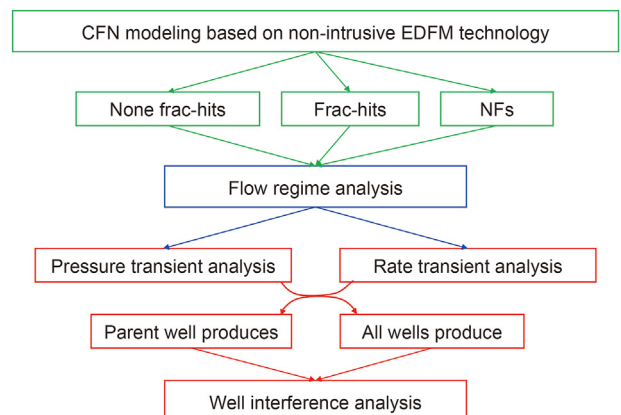


Fig. 1. Flowchart of this study.

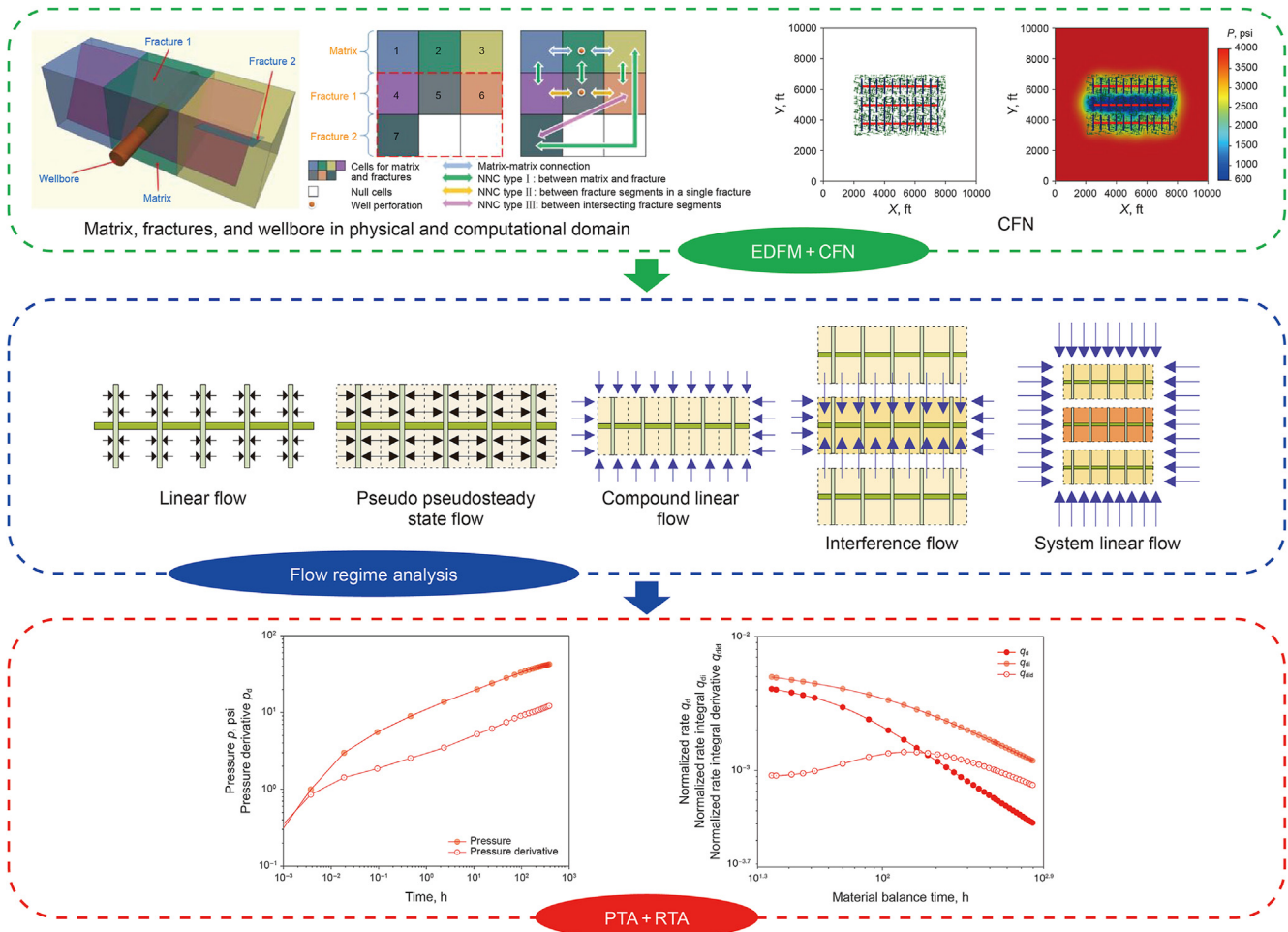


Fig. 2. General sketch of the issue under study (Modified from Xu et al., 2017).

$$T_{\text{intersecting fracture}} = \frac{\frac{k_{f1} W_{f1} L_{\text{int}}}{d_{f1}} \cdot \frac{k_{f2} W_{f2} L_{\text{int}}}{d_{f2}}}{\frac{k_{f1} W_{f1} L_{\text{int}}}{d_{f1}} + \frac{k_{f2} W_{f2} L_{\text{int}}}{d_{f2}}} \quad (3)$$

where A_f is the fracture segment area; A_c is the common face of two fracture segments; K is the matrix permeability; k_f is the fracture permeability; V is the matrix cell volume; x_n represents the distance between fracture plane and volume element; $d_{\text{Seg}i}$ is the distance between the segment i and the joint face from the individual fracture; d_{fi} is the distance between subsegment i to the fracture intersecting line.

Comparing with discrete fracture model and local grid refinement method, EDFM could provide reliable results with less computational time since EDFM applies orthogonal structured grids and does not need to use very small grids. This is beneficial for reservoir simulation with CFN especially with large number of NFs.

3. Model comparison

Eight cases are provided in this section for sensitivity analysis. Our interest here is to understand the influence of well interference, frac-hits and NF on rate and pressure transient behavior. One thing should be noticed that to emphasize the interference caused by child wells in multi-well pad, the reservoir configuration is set to be 10000 ft × 10000 ft. In this situation, boundary-dominated flow regime is hard to reach due to the low matrix permeability.

Otherwise, well interference might be covered by boundary effect which is disadvantageous to evaluate well performance. All cases serve as multi-well system each comprising three parallel horizontal wells with various fracture properties. Case 1 through Case 4 demonstrate the situations when only one parent well produces (PWP). In contrast, all wells produce (AWP) at the same time in Case 5 through Case 8. Classification and input parameters of these cases are given in Tables 1 and 2. Simulations were carried out with CMG IMEX. MFHW flows at constant BHP of 600 psi during a period of 5000 days.

- Case 1 & Case 5: Three wells are in the reservoir, shown in Fig. 3a. Each of them has eleven traditional transverse HF. There are no frac-hits or NF in the whole reservoir, which is set to be the baseline case.
- Case 2 & Case 6: Case 2 and Case 6 address the effect of frac-hits, in which well #1 and #2 are interconnected through five frac-hits without NF, while well #2 and #3 are unconnected for comparison (see Fig. 3b).

Table 1
Model classification.

Multi-well system type	HFs	Frac-hits	NFs	Frac-hits + NFs
Multi-well system when PWP	Case 1	Case 2	Case 3	Case 4
Multi-well system when AWP	Case 5	Case 6	Case 7	Case 8

Table 2
Basic input parameters.

Parameter	Value
Reservoir permeability, mD	0.0005
Reservoir porosity, %	10
Reservoir thickness, ft	100
Total compressibility, psi^{-1}	1×10^{-6}
Initial reservoir pressure, psi	4000
Bottom-hole pressure, psi	600
Wellbore radius, ft	0.25
Fracture stage	11

- Case 3 & Case 7: Case 3 and Case 7 address the effect of NF. As shown in Fig. 3c, two sets of NFs with different dominant orientations are generated based on Case 3. Input data of NF properties in Case 3 are given in Table 3.
- Case 4 & Case 8: To analyze the synthetic effect, Case 4 and Case 8 combine frac-hits and NFs together (see Fig. 3d). Other reservoir and fracture parameters keep the same values as those in the baseline case.

4. Results and discussion

The production rate and cumulative production of the parent well (Well #2) in all cases over 5000 d are shown in Fig. 4. During

Table 3
NF parameters.

NF Parameter	Value
Total number	1500
Fracture orientation (angle range), degree	70–90; 160–180
Fracture half-length, ft	100–350
Fracture permeability, mD	1.0

early time, cases with NFs (Cases 3, 4, 7, and 8) have a higher production rate than other cases (see Fig. 5). In detail, the case with frac-hits when PWP attain the highest production rate. The fracture network consists of large number of NFs and frac-hits connecting adjacent wells provide larger contact area with matrix, which effectively increases the well productivity. Besides, Fig. 4 illustrates that the case without frac-hits (Case 3) declines slower than that with frac-hits (Case 4) and becomes the largest one during late time. When AWP, although the rate of the parent well declines faster comparing with cases when PWP, the cumulative production of all wells in these cases seems higher, shown in Fig. 6.

4.1. Multi-well system when PWP

Pressure distribution in the reservoir for Cases 1 through 4 after 300 and 3000 d of production is shown in Fig. 7. As expected, well interference is absent in Case 1 due to the low matrix permeability,

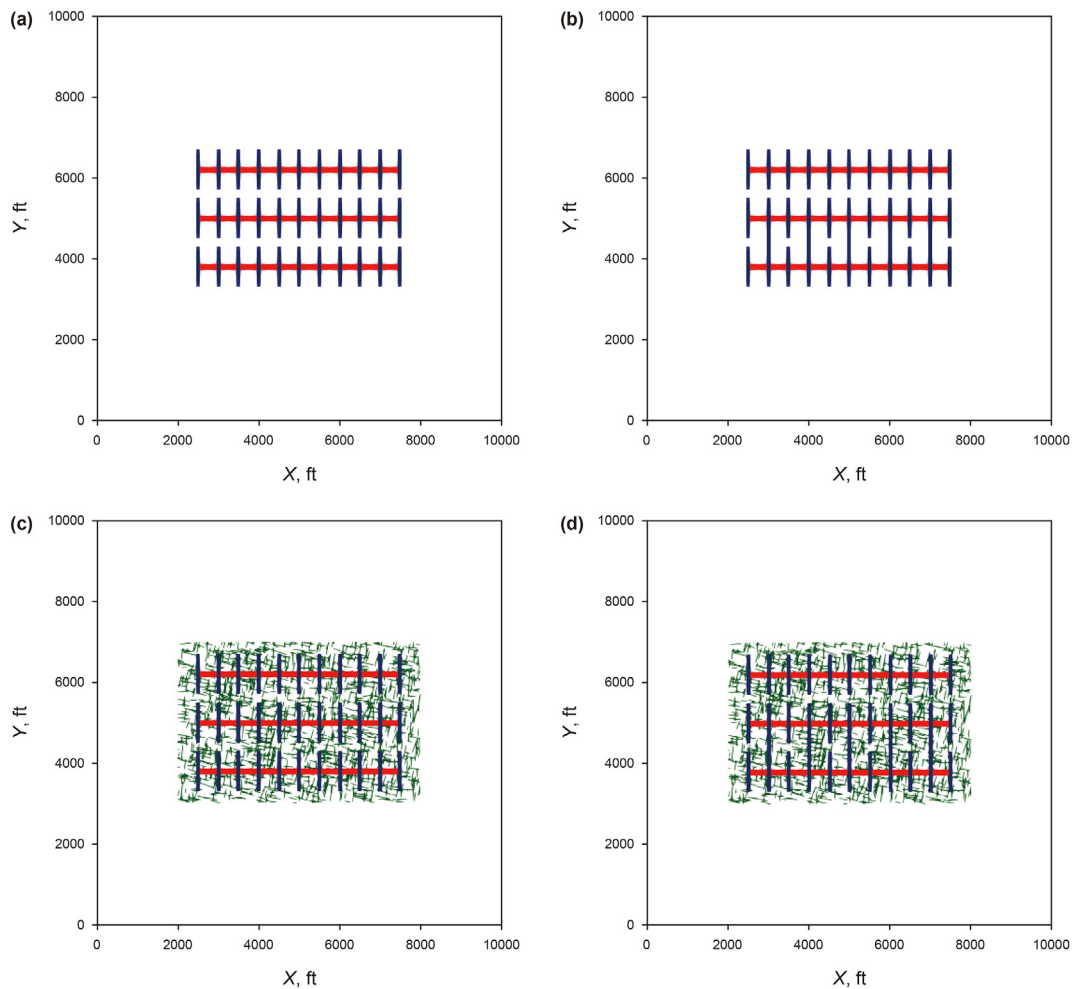


Fig. 3. Multi-well systems with frac-hits and NFs. (a) Case 1 & Case 5; (b) Case 2 & Case 6; (c) Case 3 & Case 7; (d) Case 4 & Case 8.

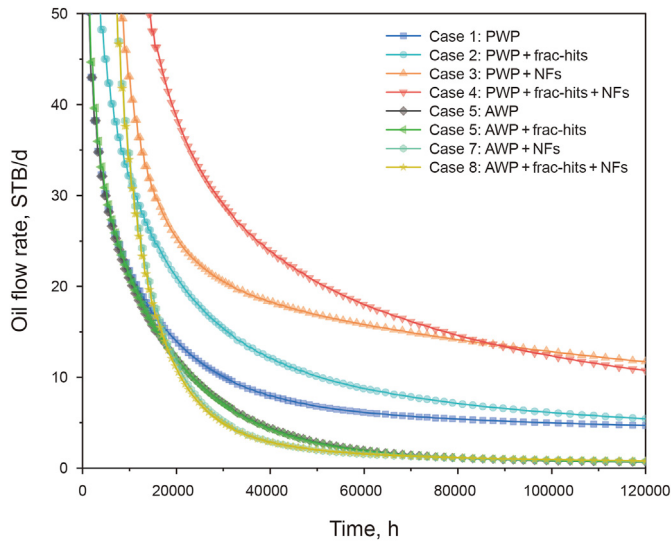


Fig. 4. Decline curve analysis (DCA) plot of well #2 during the whole producing time.

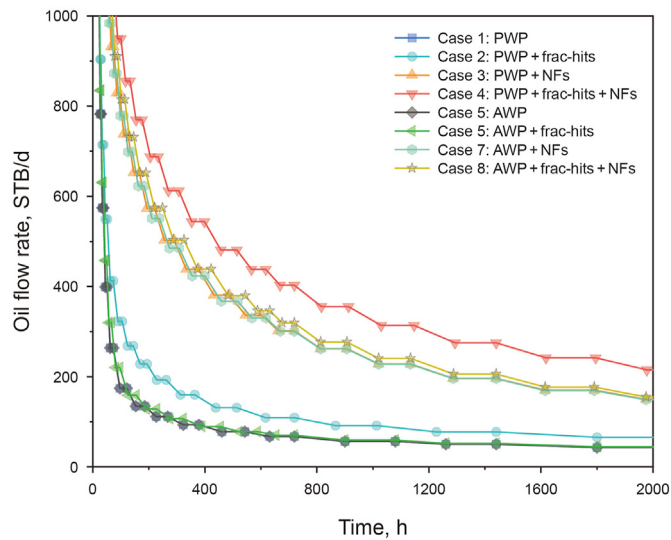


Fig. 5. DCA plot of well #2 during early time.

shown in Fig. 7a and b. Then, through the intersection between more than one HF belonging to well #1 and #2, frac-hits exist in Case 2. In this way, fluid flows from a child well to the parent well through the connected HF (Fig. 7c, d). Fig. 7e, f displays the pressure distribution of Case 3. Although the reservoir depletion around child wells still does not occur since the NF conductivity is quite small, drainage area around the parent well somehow becomes larger comparing to Cases 1 and 2. Also, the existence of NFs provides flow paths for fluids deep into the reservoir. Finally, when frac-hits (between wells #1 and #2) and NFs co-exist in the reservoir, the depletion area encompasses both the parent well and the child well (well #1) which gives the largest drainage area, shown in Fig. 7g, h. However, a limitation should be brought up that frac-hits might not be beneficial to all child wells in multi-well pad. In Cases 2 and 4, even after 3000-day production, reservoir depletion around well #3 remains indistinct comparing with that around well #2 since frac-hits improve the connectivity between well #1 and #2 while restrain the communication between #2 and #3. Even large number of NFs does not alleviate this bias. This phenomenon

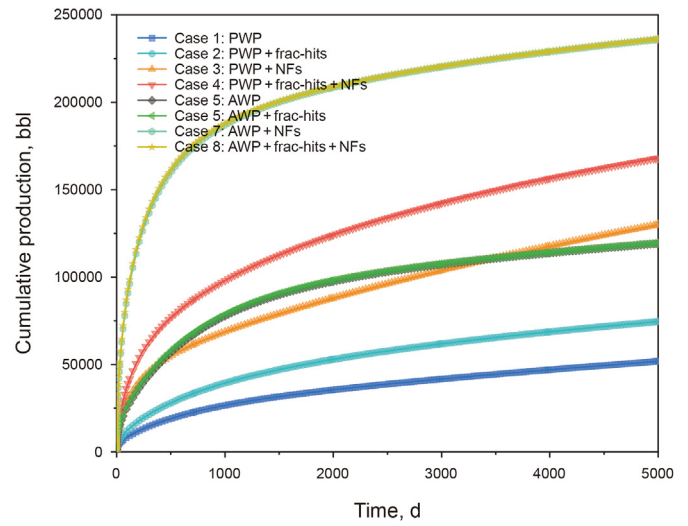


Fig. 6. Cumulative production plot of all cases.

can be observed on BHP curves and could be useful for well interference diagnosis.

Fig. 8 provides the total cumulative production of Cases 1 through 4. Comparing to the baseline case, an obvious increase in cumulative production can be observed when NFs and frac-hits exist. Moreover, in this synthetic multi-well pad, NFs show more significant influence than frac-hits. In detail, Fig. 9 displays BHP of well #1 (with frac-hits) and well #3 (without frac-hits), respectively. From this plot, it can be observed that when frac-hits between well #1 and #2 exist (Cases 2 and 4), BHP of well #1 drops nearly 1000 psi comparing with well #3, which is much closer to the BHP of well #2. Frac-hits have more influence on well #1 and NFs have stronger effect on well #3, respectively.

The log-log diagnostic plot displayed by rate normalized pressure integral (RNPI) and its derivative (RNPID) versus equivalent time is developed to identify flow regimes. When reference phase is oil or water, they are defined as

$$t_e = \frac{1}{2} \frac{Q(t)}{q(t)} \quad (4)$$

$$p_{di} = \frac{1}{t_e} \int_0^{t_e} \frac{(p_i - p(\tau))}{q(\tau)} d\tau \quad (5)$$

$$p_{did} = \frac{dp_{di}}{d \ln \tau} \quad (6)$$

where p_{di} is the rate normalized pressure integral; p_{did} is the rate normalized pressure integral derivative; t_e is the equivalent time, which is half of material balance time; Q is the cumulative production; q is the production rate; p_i is the initial pressure; p is the flowing BHP; τ is the time variable.

The flow regimes of MFHW in multi-well system considering well interference are summarized in Fig. 10. Five basic flow regimes can be identified in the baseline case (see Fig. 11), starting from fracture linear flow which displays a straight line with 0.5 slope. It is followed by pseudo pseudosteady state flow period. During this flow regime, the fluids continue to converge to fractures and the pressure drops linearly in the effective drainage area with virtual no-flow boundary (Song et al., 2011). When the SRV region

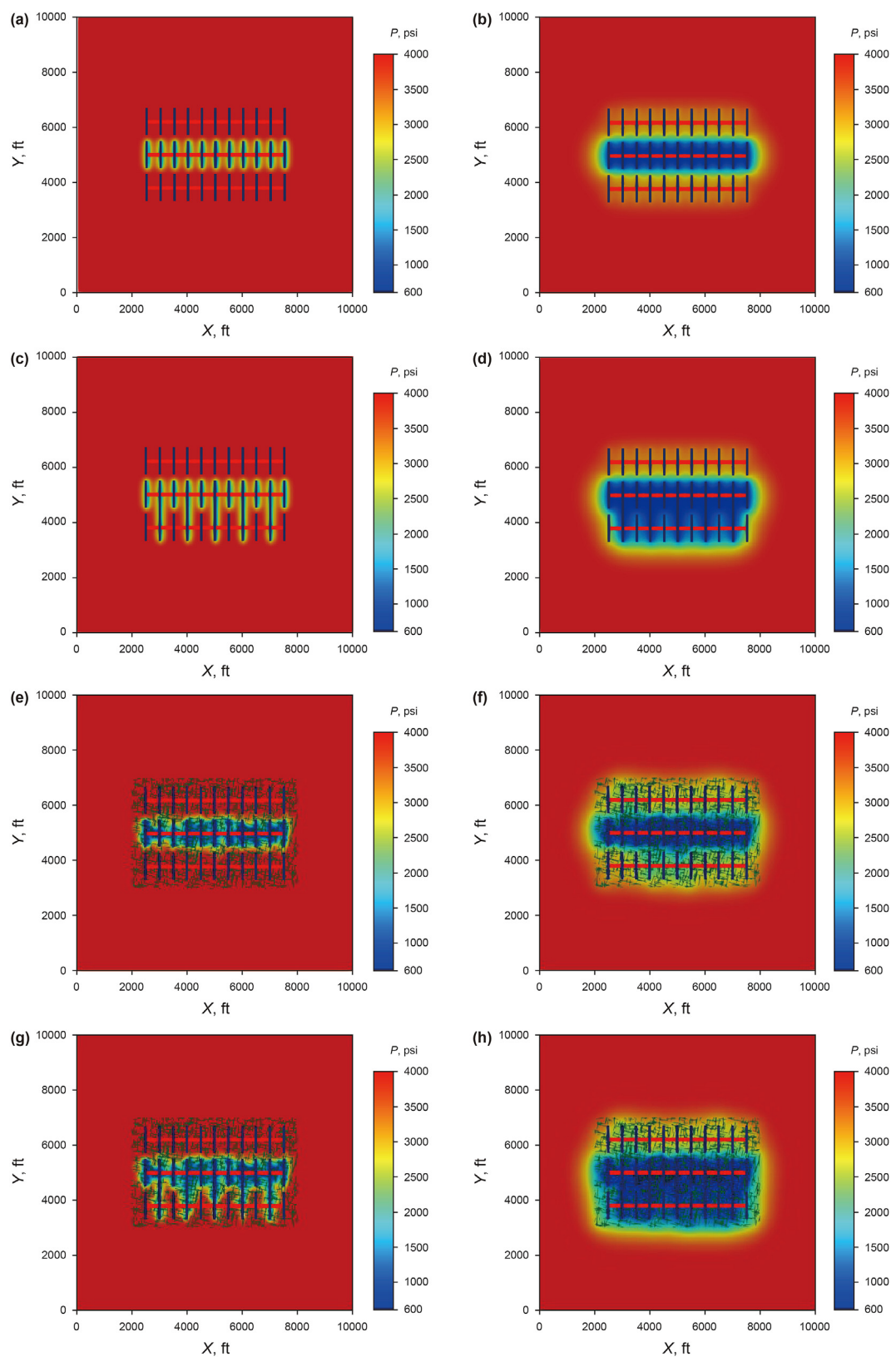


Fig. 7. Pressure distribution of Cases 1 (a, b), 2 (c, d), 3 (e, f) and 4 (g, h) after 300 (left images) and 3000 (right images) days of production.

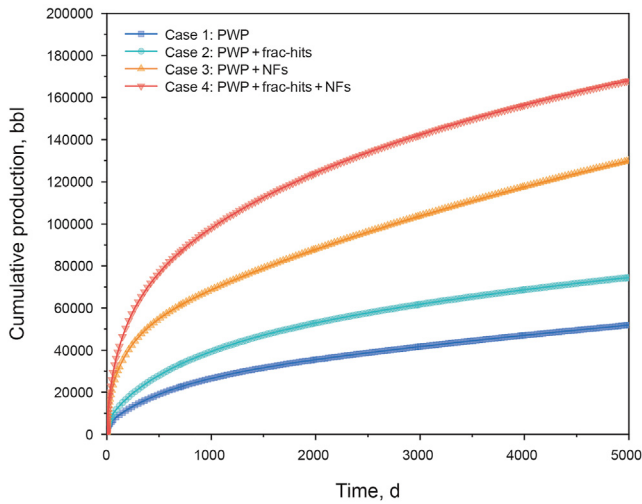


Fig. 8. Cumulative production of wells #1 and #3 of Cases 1 to 4.

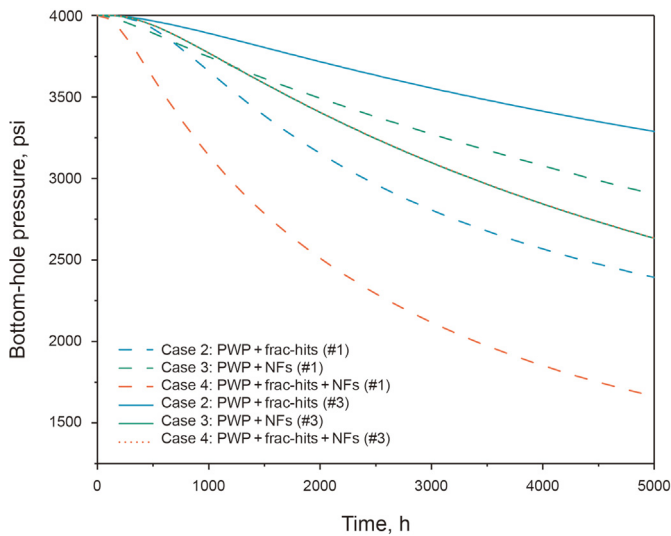


Fig. 9. BHP of well #1 and #3 of Cases 1 to 4.

gradually depletes and the fluids from the interwell region starts to flow towards the parent well, compound linear flow would occur on type curves. As the pressure further spreads, although child wells are shut-in in this section, it would still influence transient behavior of the parent well since it can provide high permeability flowing channel. Once these HFs of child wells are sensed, the parent well would reach well interference flow regime with the slope between 0 and 1. Later, fluids inside the SRV region of all wells

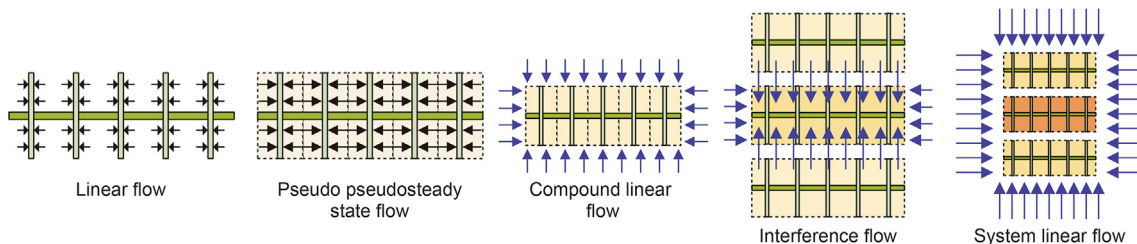


Fig. 10. Flow regime in multi-well system considering well interference.

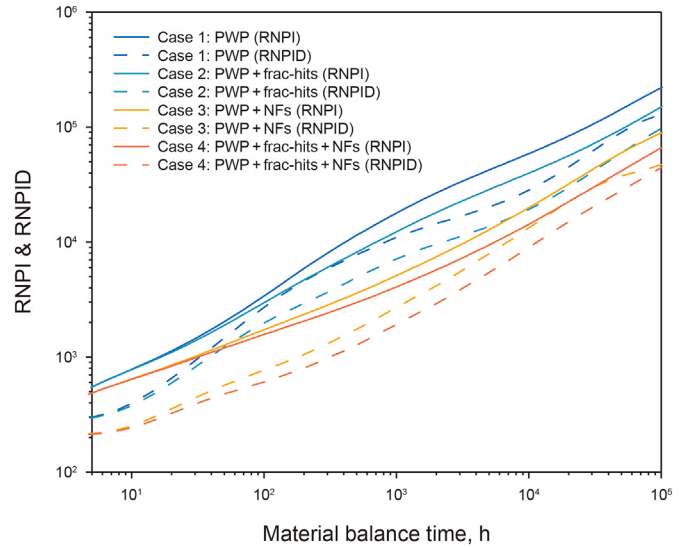


Fig. 11. The log–log plot of MFHW in multi-well system considering reservoir complexity and well interference when PWP.

would deplete and system linear flow can be observed.

When reservoir complexities (e.g. frac-hits and NF) occur, there would be some deviations from the classic flow regime behavior listed above. For example, the duration of pseudo pseudosteady state flow becomes shorter since frac-hits help connecting well #1 and #2. Instead, fracture interference flow between the fracture linear flow and the compound linear flow can be observed in Case 2. Another interesting finding is that NFs seem to have stronger impact on simulation results than that of frac-hits. The CFN comprising HFs from three wells and two sets of NFs in this multi-well pad significantly enlarge the drainage area of the parent well (Cases 3 and 4). As a result, the transition of well interference flow between variable linear flows seems to be quite smooth.

Figs. 12 and 13 display the pressure normalized rate (PNR), pressure normalized rate integral (PNRI) and its derivative (PNRID). PNR, PNRI and PNRID are given by

$$q_d = \frac{q(\tau)}{p_i - p_{wf}(\tau)} \quad (7)$$

$$q_{di} = \frac{1}{t_e} \int_0^{t_e} \frac{q(\tau)}{p_i - p_{wf}(\tau)} d\tau \quad (8)$$

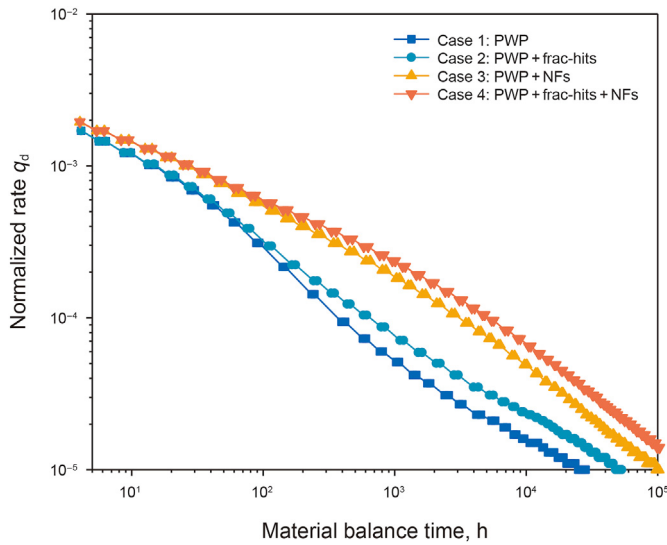


Fig. 12. PNR of Cases 1 to 4.

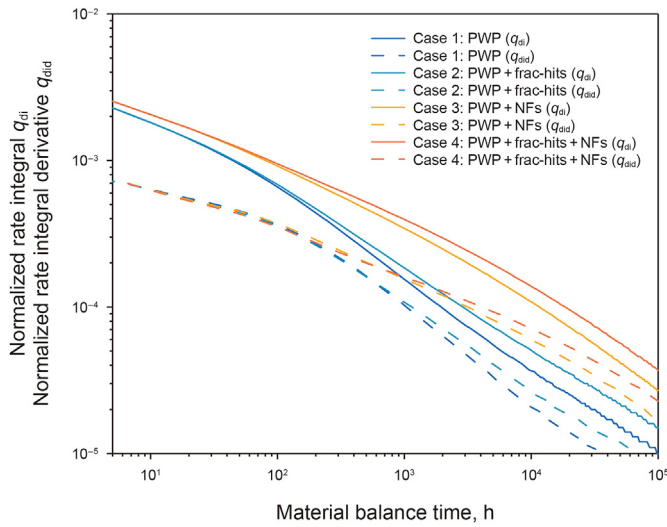


Fig. 13. PNRI and PNRID of Cases 1 to 4.

$$q_{diid} = \frac{\partial}{\partial \ln t_e} \left[\frac{1}{t_e} \int_0^{t_e} \frac{q(\tau)}{p_i - p_{wf}(\tau)} d\tau \right] \quad (9)$$

where q_d is the pressure normalized rate; q_{di} is the pressure normalized rate integral; q_{diid} is the pressure normalized rate integral derivative; $p_{wf}(\tau)$ is the BHP at time τ .

Due to extremely low matrix permeability in this synthetic large range reservoir, it is hard to reach boundary-dominated flow. As production begins, we can see similar trends for cases when PWP until pseudo pseudosteady state flow dominates the response of Case 1. Then, it can be identified that the Blasingame plots (Blasingame et al., 1991) of these four cases can be classified into two categories based on different reservoir complexities (i.e. frac-hits and NFs). Note that NFs can cause apparent deviations from the baseline case since early-time production, while frac-hits make less contribution than that of NFs.

4.2. Multi-well system when AWP

The basic properties of reservoir and fractures of Cases 5 through 8 are identical to those of Cases 1 through 4, respectively. The difference between them is that child wells produce in Cases 5 to 8 instead of shut-in in the former cases. Pressure distribution in the reservoir for Cases 5 through 8 after 300 days of production is shown in Fig. 14a, c, e, g. For cases when AWP, the impact of frac-hits becomes hard to recognize no matter NFs exist (Cases 7 and 8) or not (Cases 5 and 6). Both of fracture interference and well interference caused by frac-hits are difficult to visualize. On the contrary, reservoir depletion around all three wells seems distinct when NFs exist. Fig. 14b, d, f, h displays the drainage area of Cases 5 through 8 after 3000 days of production. The drainage area of Cases 7 and 8 (with NFs) seems to be a little bit bigger than that of Cases 5 and 6 (without NFs). This is because NFs only concentrate around the parent well and child wells in these cases. The reservoir depletion area would be larger when the entire reservoir is covered by NFs.

The log–log plots of MFHW in multi-well system when AWP are shown in Fig. 15. Flow regimes including fracture linear flow, pseudo pseudosteady state flow, compound linear flow regime and interference flow which have been mentioned above can be observed. Pressure depletes faster in the multi-well system since AWP at the same time. Therefore, system linear flow is substituted by pseudosteady state flow regime with unit slope. When AWP, there might be some slightly deviation during pseudo pseudosteady state flow regime due to the existence of frac-hits. However, it is hard to recognize and could be neglected during type curve analysis. In contrast, the impact of NFs on interference flow connecting different linear flows is obvious comparing with that of frac-hits. PNR, PNRI and PNRID of cases when AWP are shown in Fig. 16. For cases when PWP, curves can be classified into two categories based on different reservoir complexities including frac-hits and NFs, and the curves start to separate from the beginning of early time flow regime since pseudo pseudosteady state flow dominates the response of Case 5. Fig. 17a displays that there seems to exist minor differences between two different child wells (well #1 and well #3) on log–log plot since well #1 are connected to the parent well (well #2) through frac-hits. The deviation caused by well interference becomes more obvious when NFs exist (see Fig. 17b, c).

5. Field case study

The field data are from MFHWs of Block #Q in the tight oil reservoir in China. Application of horizontal well drilling and hydraulic fracturing technology enables economic production of Block #Q, and it was put into exploitation since 2014. Firstly, history matching is conducted before well interference evaluation. The total liquid rates of the numerical model are the same as the field data (Fig. 18a), the matching result of oil rates of Well A is shown in Fig. 18b. Pressure distribution of multi-well pad in May 2018 is shown in Fig. 19.

After history matching, the RTA and PTA plots are developed to analyze the of transient rate/pressure behavior. A newly drilled MFHW (Well B) has been opened for production since Jan 31st, 2018, which is about 700 ft away from Well A. Based on the BHP data of Well A, PTA plot is obtained, as shown in Fig. 20. It is observed that the pressure and pressure derivative quickly decrease after linear flow regime due to the well interference from the Well B. To further compare the impact of well interference on pressure and pressure derivative curves, a new case is established, and Well B is shut in. It is obvious that the well interference is missing in the PTA plot and long linear flow can be observed for the

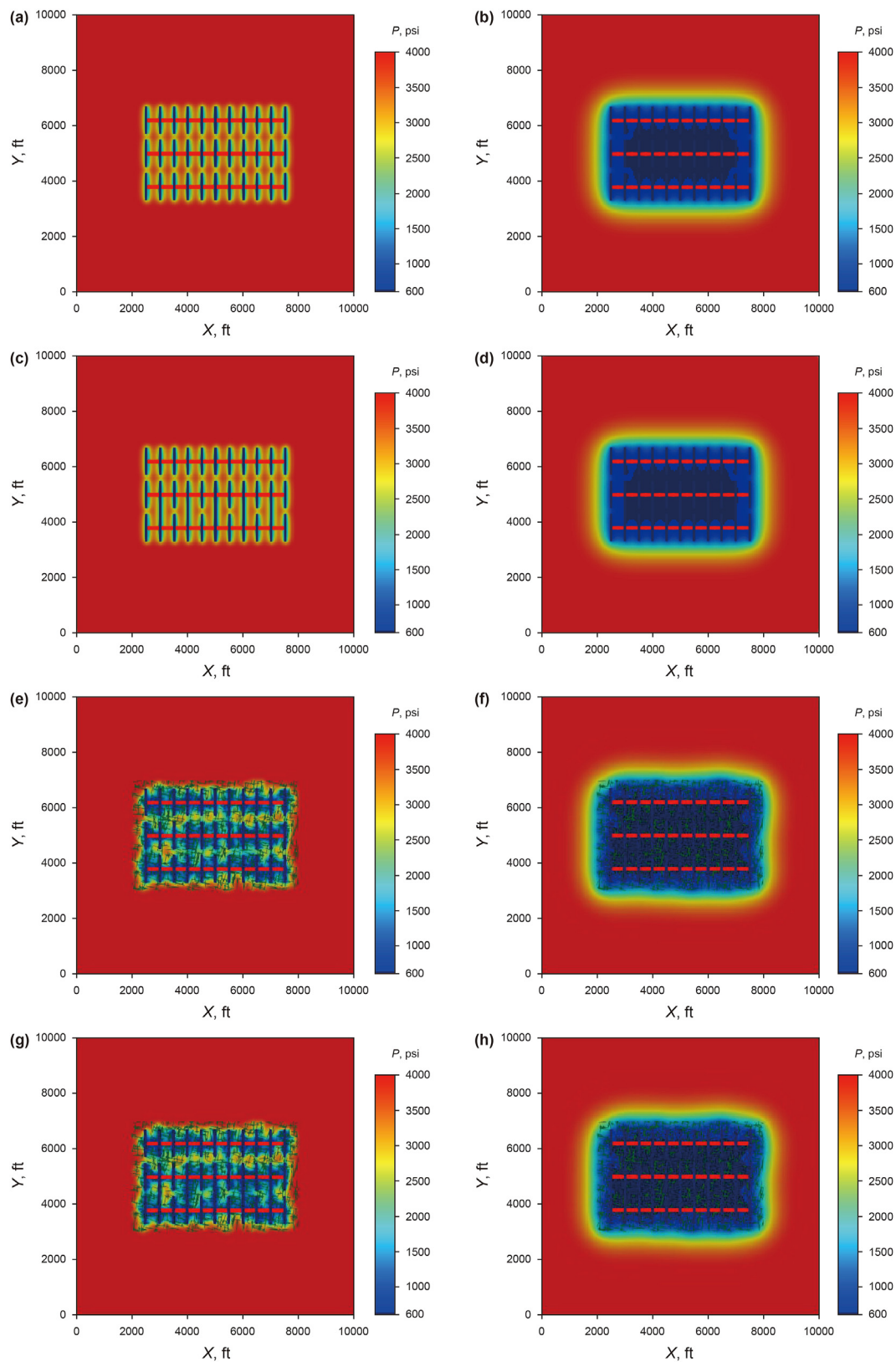


Fig. 14. Pressure distribution of Cases 5 (a, b), 6 (c, d), 7 (e, f), and 8 (g, h) after 300 (left images) and 3000 (right images) days of production.

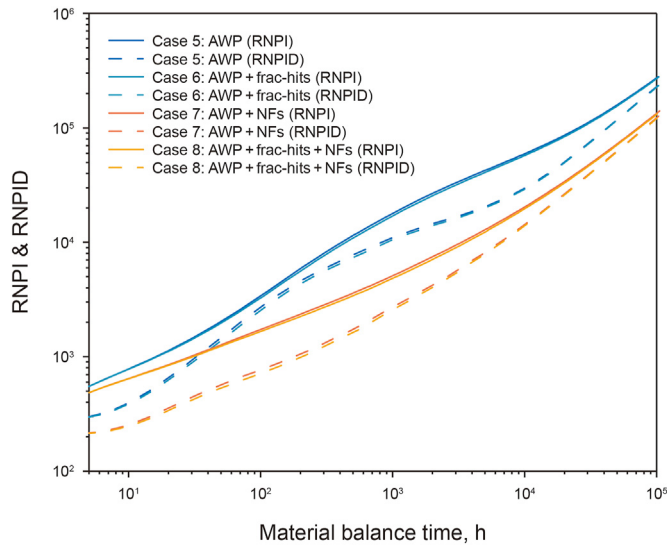


Fig. 15. The log–log plot of multi-well system considering reservoir complexity and well interference when AWP.

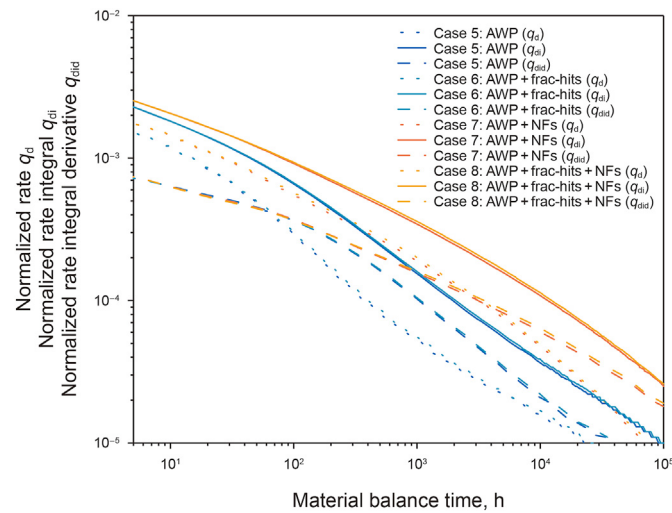
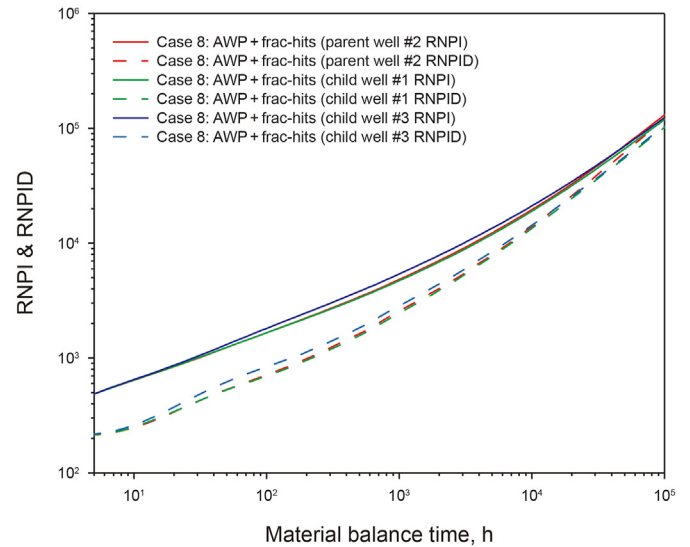
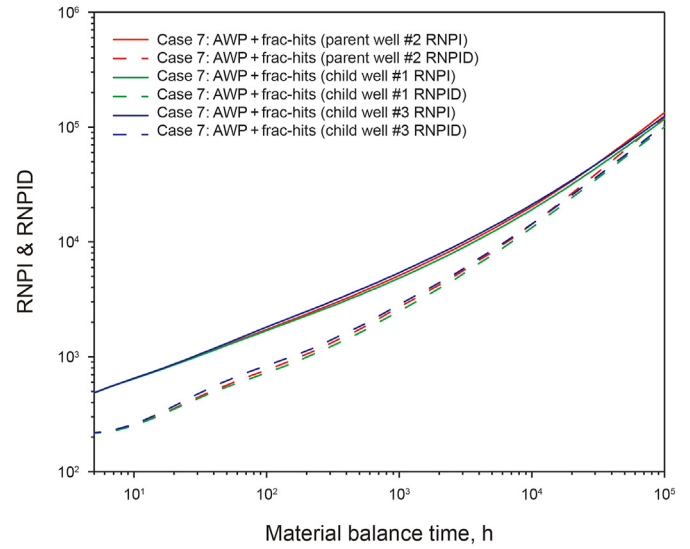
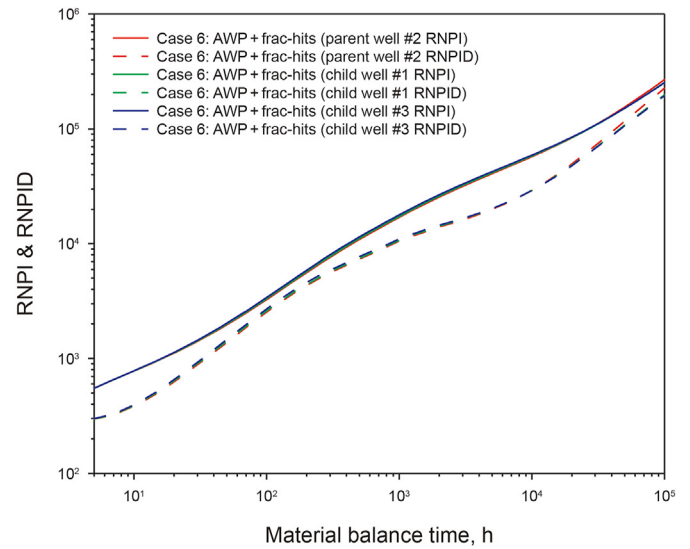


Fig. 16. Blasingame plot of multi-well system considering reservoir complexity and well interference when AWP.

new case ignoring well interference, shown in Fig. 21.

For the case with two MFHWs, the linear flow behavior is affected due to the interference from adjacent Well B on the log–log plot (Fig. 22). Both the RNPI and RNPID increase significantly after fracture linear flow regime. In contrast, the curves would decrease quickly due to this interference during late time on Blasingame plot, as shown in Fig. 23.

In unconventional oil and gas reservoirs, multi-well pads have become an economic and environmental way to develop hydrocarbon fluids. Multiple MFHWs are densely distributed in a well pad, and interference among wells could have strong influence on pressure and rate transient behavior so that it cannot be ignored for PTA and RTA analysis. Furthermore, the combination of PTA and RTA can provide a more reliable evaluation.

6. Summary and conclusions

A flexible numerical integrated approach for fracture

Fig. 17. The log–log plot of wells #1, #2 and #3 of Case 6 (a) Case 7 (b) and Case 8 (c).

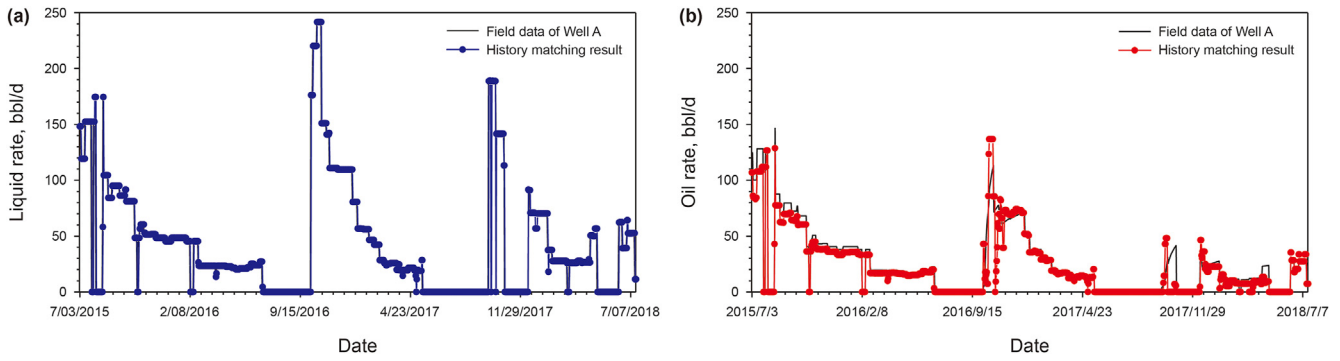


Fig. 18. History matching results of Well A. (a) Liquid rate; (b) Oil rate.

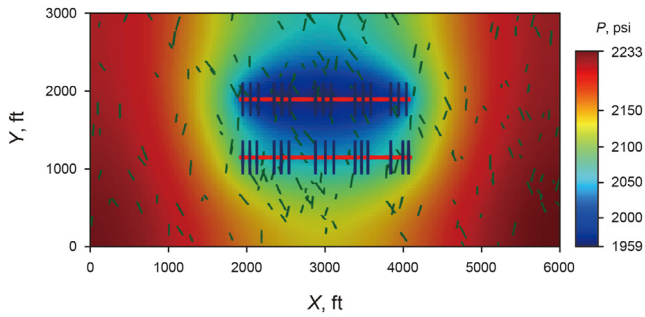


Fig. 19. Pressure distribution of multi-well pad in May 2018.

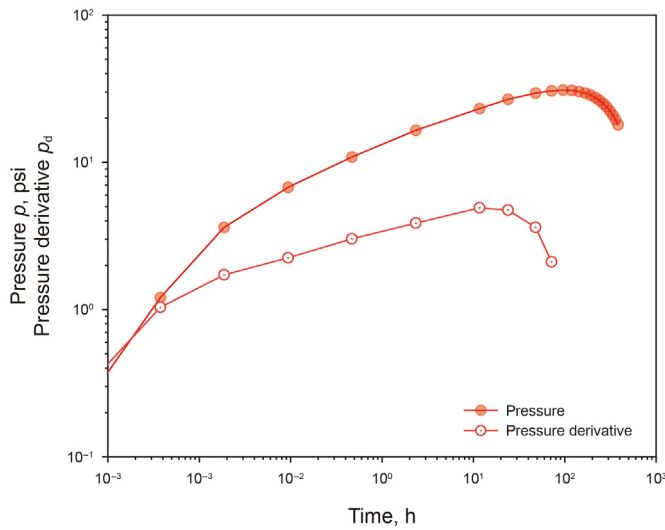


Fig. 20. PTA plot of Well A considering well interference.

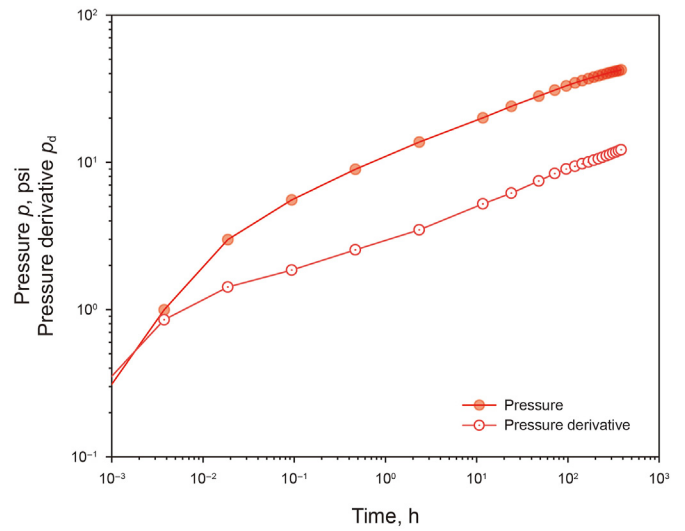


Fig. 21. PTA plot of Well A ignoring well interference.

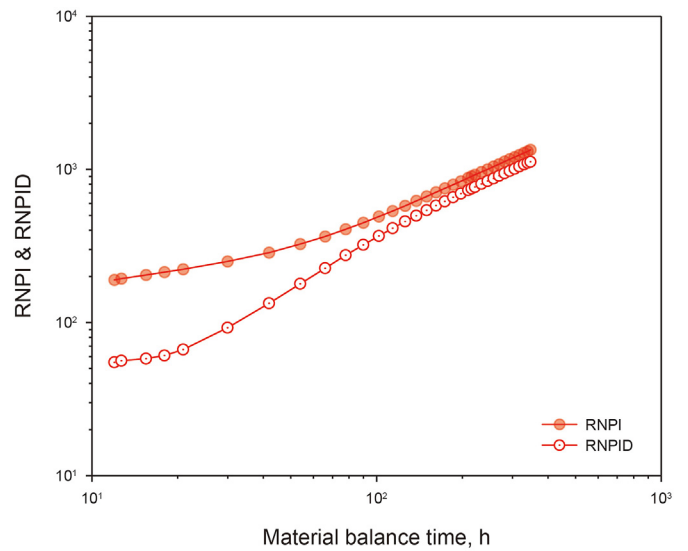


Fig. 22. The log–log plot of Well A.

interference and well interference diagnosis combining PTA and RTA has been established in this paper. Then, CFN can be easily and efficiently handled through EDFM technology. The following conclusions could be drawn:

- (1) Interference from surrounding producers results in the appearance of new flow regimes including compound linear flow and interference flow on log–log plot. Five basic flow regimes including linear flow, pseudosteady state flow, compound linear flow, interference flow, and system linear flow can be observed on type curves of an MFWH in multi-

well system. NFs and frac-hits would have different effect on type curves.

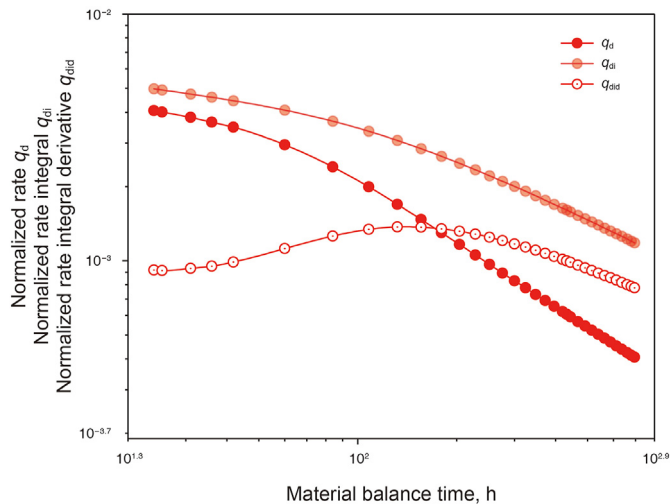


Fig. 23. Blasingame plot of Well A.

- (2) Distinctive increase in cumulative production could be obtained in cases with NFs and frac-hits. In general, NFs seem to show more evident influence compared with frac-hits. When NFs and frac-hits exist in the reservoir together, frac-hits have more influence on well #1 (with frac-hits) and NFs have stronger effect on well #3 (without frac-hits), respectively.
- (3) On the log–log plot, slight deviation during pseudosteady state flow caused by frac-hits is hard to identify for cases when AWP. In contrast, the influence of NFs on interference flow is more distinct.
- (4) Boundary-dominated flow is hard to reach since the permeability of unconventional reservoir is quite low. Blasingame plots can be divided into two types according to different CFN patterns.
- (5) It shows that the impact of frac-hits on fracture interference and well interference is hard to visualize in pressure distribution. Compared with frac-hits, reservoir depletion seems obvious when NFs exist.

The proposed approach can achieve better reservoir evaluation based on the new features observed in the novel model. The combination of PTA and RTA can help reduce the uncertainty and improve the accuracy of well interference interpretation using both the field pressure and rate data.

Acknowledgements

The authors are grateful to the financial support from China Postdoctoral Science Foundation (2022M712645) and Opening Fund of Key Laboratory of Enhanced Oil Recovery (Northeast Petroleum University), Ministry of Education (NEPU-EOR-2021-03). We would also like to acknowledge Computer Modeling Group Ltd., KAPPA Engineering, and Sim Tech LLC for providing the CMG, Topaze, and EDFM software, respectively. The authors would like to thank Tuha Oilfield, CNPC for providing the data and their permission to publish this material.

References

Ajayi, A., Cox, R., Schmitt, B., Elliott, B., 2016. Quantifying changes in hydraulic fracture properties using a multi-well integrated discrete fracture network (DFN) and reservoir simulation model in an unconventional wolfcamp fm., midland basin, west Texas. In: SPE/AAPG/SEG Unconventional Resources

Technology Conference. Society of Petroleum Engineers. <https://doi.org/10.15530/URTEC-2016-2455780>.

Al-Kabbawi, F.A.A., 2022. The optimal semi-analytical modeling for the infinite-conductivity horizontal well performance under rectangular bounded reservoir based on a new instantaneous source function. *Petroleum*.

Al-Khamis, M., Ozkan, E., Raghavan, R., 2001. Interference testing with horizontal observation wells. In: SPE Annual Technical Conference and Exhibition. Society of Petroleum Engineers. <https://doi.org/10.2118/71581-MS>.

Blasingame, T.A., McCray, T.L., Lee, W.J., 1991. Decline curve analysis for variable pressure drop/variable flowrate systems. In: SPE Gas Technology Symposium. Society of Petroleum Engineers. <https://doi.org/10.2118/21513-MS>.

Chen, Z., Liao, X., Zeng, L., 2020. Pressure transient analysis in the child well with complex fracture geometries and fracture hits by a semi-analytical model. *J. Pet. Sci. Eng.* 191 (2020), 107119. <https://doi.org/10.1016/j.petrol.2020.107119>.

Driscoll, V.J., 1963. Use of well interference and build-up data for early quantitative determination of reserves, permeability and water influx. *J. Petrol. Technol.* 15 (10), 1127–1136. <https://doi.org/10.2118/427-PA>.

Elkins, L.F., 1953. Reservoir performance and well spacing, spraberry trend area field of west Texas. *J. Petrol. Technol.* 5 (7), 177–196. <https://doi.org/10.2118/953177-G>.

Fiallos, M.X., Yu, W., Ganjanesh, R., Kerr, E., Sepehrmoori, K., Miao, J., Ambrose, R., 2019. Modeling interwell interference due to complex fracture hits in eagle ford using edfm. In: International Petroleum Technology Conference. <https://doi.org/10.2523/IPTC-19468-MS>.

Gao, D., Liu, Y., Pan, S., Wang, J., Zhou, X., 2020. Longitudinal interference analysis of shale gas multi-stage fracturing horizontal wells upon high-precision pressure test. *Energy Sci. Eng.* 8 (7), 2387–2401. <https://doi.org/10.1002/ese3.671>.

Gao, D., Liu, Y., Wang, D., Han, G., 2019. Numerical analysis of transient pressure behaviors with shale gas mfws interference. *Energies* 12 (2), 262. <https://doi.org/10.3390/en12020262>.

Guindon, L., 2015. Determining interwell connectivity and reservoir complexity through fracturing pressure hits and production-interference analysis. *J. Can. Pet. Technol.* 54 (2), 88–91. <https://doi.org/10.2118/0315-088-JCPT>.

He, Y., Qiao, Y., Qin, J., Tang, Y., Wang, Y., Chai, Z., 2022. A novel method to enhance oil recovery by inter-fracture injection and production through the same multifractured horizontal well. *J. Energy Resour. Technol.* 144 (4), 043005. <https://doi.org/10.1115/1.4051623>.

He, Y., Qin, J., Cheng, S., Chen, J., 2020. Estimation of fracture production and water breakthrough locations of multi-stage fractured horizontal wells combining pressure-transient analysis and electrical resistance tomography. *J. Pet. Sci. Eng.* 194, 107479. <https://doi.org/10.1016/j.petrol.2020.107479>.

Houali, A., Tiab, D., 2005. Analysis of interference testing of horizontal wells in an anisotropic medium. In: Canadian International Petroleum Conference. Petroleum Society of Canada. <https://doi.org/10.2118/2005-066>.

Issaka, M.B., Ambastha, A.K., 1997. Interpretation of estimated horizontal well lengths' from interference test data. *J. Can. Pet. Technol.* 36 (6), 39–47. <https://doi.org/10.2118/97-06-03>.

Jacobs, T., 2017. Oil and gas producers find frac hits in shale wells a major challenge. *J. Petrol. Technol.* 69 (4), 29–34. <https://doi.org/10.2118/0417-0029-JPT>.

Lawal, H., Jackson, G., Abolo, N., Flores, C., 2013. A novel approach to modeling and forecasting frac hits in shale gas wells. In: EAGE Annual Conference & Exhibition Incorporating SPE Europec. Society of Petroleum Engineers. <https://doi.org/10.2118/164898-MS>.

Malekzadeh, D., 1992. Deviation of horizontal well interference testing from the exponential integral solution. In: SPE Rocky Mountain Regional Meeting. Society of Petroleum Engineers. <https://doi.org/10.2118/24372-MS>.

Malekzadeh, D., Tiab, D., 1991. Interference testing of horizontal wells. In: SPE Annual Technical Conference and Exhibition. Society of Petroleum Engineers. <https://doi.org/10.2118/22733-MS>.

Miao, J., Yu, W., Xia, Z., Zhao, W., Xu, Y., Sepehrmoori, K., 2018. An easy and fast edfm method for production simulation in shale reservoirs with complex fracture geometry. *American Rock Mechanics Association*. <https://onepetro.org/ARMADFNE/proceedings/DFNE18/3-DFNE18/DO33S018R002/122764>.

Mohammed, I., Olayiwola, T.O., Alkathim, M., Awotunde, A.A., Alafnan, S.F., 2020. A review of pressure transient analysis in reservoirs with natural fractures, vugs and/or caves. *Petrol. Sci.* 18 (1), 154–172. <https://doi.org/10.1007/s12182-020-00505-2>.

Nobakht, M., Clarkson, C.R., 2012. Multiwell analysis of multifractured horizontal wells in tight/shale gas reservoirs. In: SPE Canadian Unconventional Resources Conference. Society of Petroleum Engineers. <https://doi.org/10.2118/162831-MS>.

Qin, J., Cheng, S., Li, P., He, Y., Lu, X., Yu, H., 2019. Interference well–test model for vertical well with double–segment fracture in a multi–well system. *J. Pet. Sci. Eng.* 183, 106412. <https://doi.org/10.1016/j.petrol.2019.106412>.

Qin, J., Xu, Y., Tang, Y., Liang, R., Zhong, Q., Yu, W., Sepehrmoori, K., 2022. Impact of complex fracture networks on rate transient behavior of wells in unconventional reservoirs based on embedded discrete fracture model. *J. Energy Resour. Technol.* 144 (8), 083007. <https://doi.org/10.1115/1.4053135>.

Sardinha, C.M., Petr, C., Lehmann, J., Pyecroft, J.F., Merkle, S., 2014. Determining interwell connectivity and reservoir complexity through frac pressure hits and production interference analysis. In: SPE/CSUR Unconventional Resources Conference – Canada. Society of Petroleum Engineers. <https://doi.org/10.2118/171628-MS>.

Song, B., Economides, M.J., Ehlig-Economides, C.A., 2011. Design of multiple transverse fracture horizontal wells in shale gas reservoirs. In: SPE Hydraulic

- Fracturing Technology Conference. Society of Petroleum Engineers. <https://doi.org/10.2118/140555-MS>.
- Tang, H., Yan, B., Chai, Z., Zuo, L., Killough, J., Sun, Z., 2019. Analyzing the well-interference phenomenon in the eagle ford shale/austin chalk production system with a comprehensive compositional reservoir model. *SPE Reservoir Eval. Eng.* 22 (3), 827–841. <https://doi.org/10.2118/191381-PA>.
- Tripoppoom, S., Yu, W., Sepehrnoori, K., Miao, J., 2019. Application of assisted history matching workflow to shale gas well using edfm and neural network-Markov chain Monte Carlo algorithm. In: SPE/AAPG/SEG Unconventional Resources Technology Conference. Unconventional Resources Technology Conference. <https://doi.org/10.15530/urtec-2019-659>.
- Wang, J., Jia, A., Wei, Y., Qi, Y., Dai, Y., 2018. Laplace-domain multiwell convolution for simulating pressure interference response of multiple fractured horizontal wells by use of modified stehfest algorithm. *J. Pet. Sci. Eng.* 161, 231–247. <https://doi.org/10.1016/j.petrol.2017.11.074>.
- Wei, M., Duan, Y., Dong, M., Fang, Q., Dejam, M., 2019. Transient production decline behavior analysis for a multi-fractured horizontal well with discrete fracture networks in shale gas reservoirs. *J. Porous Media* 22 (3), 343–361. <https://doi.org/10.1615/JPorMedia.2019028982>.
- Xiao, C., Dai, Y., Tian, L., Lin, H., Zhang, Y., Yang, Y., Hou, T., Deng, Y., 2018. A semianalytical methodology for pressure-transient analysis of multiwell-pad-production scheme in shale gas reservoirs, part 1: new insights into flow regimes and multiwell interference. *SPE J.* 23 (3), 885–905. <https://doi.org/10.2118/187958-PA>.
- Xiao, C., Tian, L., Zhang, Y., Hou, T., Yang, Y., Deng, Y., Wang, Y., Chen, S., 2017. A novel approach to detect interacting behavior between hydraulic fracture and natural fracture by use of semianalytical pressure-transient model. *SPE J.* 22 (6), 1834–1855. <https://doi.org/10.2118/187954-PA>.
- Xu, Y., 2015. Implementation and Application of the Embedded Discrete Fracture Model (EDFM) for Reservoir Simulation in Fractured Reservoirs. The University of Texas at Austin [Master Thesis]. <http://hdl.handle.net/2152/34216>.
- Xu, Y., Cavalcante, J.S.A., Yu, W., Sepehrnoori, K., 2017. Discrete-fracture modeling of complex hydraulic-fracture geometries in reservoir simulators. *SPE Reservoir Eval. Eng.* 20 (2), 403–422. <https://doi.org/10.2118/183647-PA>.
- Xu, Y., Sepehrnoori, K., 2019. Development of an embedded discrete fracture model for field-scale reservoir simulation with complex corner-point grids. *SPE J.* 24 (4), 1552–1575. <https://doi.org/10.2118/195572-PA>.
- Xu, Y., Yu, W., Li, N., Lolon, E., Sepehrnoori, K., 2018. Modeling well performance in piceance basin niobrara formation using embedded discrete fracture model. In: SPE/AAPG/SEG Unconventional Resources Technology Conference. Unconventional Resources Technology Conference. <https://doi.org/10.15530/URTEC-2018-2901327>.
- Yadav, H., Motealleh, S., 2017. Improving quantitative analysis of frac-hits and refracs in unconventional plays using RTA. In: SPE Hydraulic Fracturing Technology Conference and Exhibition. Society of Petroleum Engineers. <https://doi.org/10.2118/184812-MS>.
- Yu, W., Wu, K., Zuo, L., Miao, J., Sepehrnoori, K., 2019. Embedded discrete fracture model assisted study of gas transport mechanisms and drainage area for fractured shale gas reservoirs. In: SPE/AAPG/SEG Unconventional Resources Technology Conference. <https://doi.org/10.15530/urtec-2019-552>.
- Yu, W., Xu, Y., Weijermars, R., Wu, K., Sepehrnoori, K., 2018. A numerical model for simulating pressure response of well interference and well performance in tight oil reservoirs with complex-fracture geometries using the fast embedded-discrete-fracture-model method. *SPE Reservoir Eval. Eng.* 21 (2), 489–502. <https://doi.org/10.2118/184825-PA>.
- Zhuang, H., 2012. Dynamic Well Testing in Petroleum Exploration and Development. Elsevier Inc, Amsterdam, The Netherlands. <https://doi.org/10.1016/B978-0-12-397161-6.02001-5>.